journal of the mechanical behavior of biomedical materials xxx (xxxx) xxx

Contents lists available at ScienceDirect

Journal of the Mechanical Behavior of Biomedical Materials

journal homepage: www.elsevier.com/locate/jmbbm

Research paper

Effect of haptic geometry in C-loop intraocular lenses on optical quality

I. Cabeza-Gil [a,*], J. Pérez-Gracia [b], L. Remón [b], B. Calvo [a,c]

[a] Aragón Institute of Engineering Research (I3A), University of Zaragoza, Spain
[b] Departamento de Física Aplicada, University of Zaragoza, Spain
[c] Centro de Investigación Biomédica en Red en Bioingenieria, Biomateriales y Nanomedicina (CIBER-BBN), Spain

ARTICLE INFO

Keywords:
Biomechanical stability
IOLs
Finite element
Optical performance
Haptic design
Hydrophobic acrylate

ABSTRACT

The biomechanical stability of intraocular lenses (IOLs) must achieve high-quality optical performance and clinical outcomes after cataract surgery. For this reason, the quality and performance features of the IOLs should be previously analysed following the Standard ISO 11979-2 and ISO 11979-3. The ISO 11979-3 tries to reproduce the behaviour of the IOL in the capsular bag by compressing the lens between two clamps. With this test, it has been demonstrated that the haptic design is a crucial factor to obtain biomechanical stability. Hence, the main goal of this study was to design an aberration-free aspheric IOL and to study the influence of haptic geometry on the optical quality. For that purpose, 5 hydrophobic IOLs with different haptic design were manufactured and their biomechanical stability was compared experimentally and numerically. The IOLs were classified as stiff and flexible designs depending on their haptic geometry. The biomechanical response was measured by means of the compression force, the axial displacement, the angle of contact or contact area, the decentration, the tilt and the strain energy. The results suggest that *in vitro* and *in silico* compression tests present similar responses for the IOLs analysed. Furthermore, the flexible IOL designs presented better biomechanical stability than stiff designs. These results were correlated with the optical performance, where the optical quality decreases with worst biomechanical stability. This numerical methodology provides an indisputable advance regarding IOL designs, leading to reduce costs by exploring a feasible space of solutions during the product design process and prior to manufacturing.

1. Introduction

The mechanical stability of intraocular lenses (IOLs) inside the capsular bag is a critical factor that affects the optical performance and clinical outcomes after cataract surgery. The biomechanical response is essential in IOLs which demand a fixed optic position, as for example, premium IOLs such as multifocal, toric, and aspheric designs (Alió et al., 2013; Pérez-Merino and Marcos, 2018; Zvorničanin and Zvorničanin, 2018). IOL axial displacement, rotation, decentration and tilt can result in residual refractive errors and other complications, requiring explantation or repositioning of the IOL in certain cases (Chan et al., 2010).

Intraocular lens stability depends on some factors such as: capsulorhexis size (Nagy et al., 2011), IOL diameters versus capsular bag diameter (Vounotrypidis et al., 2018), IOL material properties (Chua et al., 2012; Bozukova et al., 2013), and above all, haptic design (Wirtitsch et al., 2004; Crnej et al., 2011; Choi et al., 2018). The main function of the haptics is to offer proper positional stability, avoiding tilt, decentration, or rotation of the optic (Garzón et al., 2015; Miháltz et al., 2018). There are different haptics designs which depend on the shape such as plate and open-loop style (Chang, 2008; Prinz et al., 2011; Bozukova et al., 2015). However, the effectiveness of one against the other has not yet been proved, being the open-loop style the most common design. Furthermore, the shape of the haptics can be planar (0-degree angle); step-vaulted (having an offset from the optical plane); and angulated (forming an angle relative to the optic plane). Several clinical studies have evaluated mechanical stability with each of these designs (Schmidbauer et al., 2002; Vock et al., 2007).

In order to reliably predict the postoperative optical performance and the mechanical behaviour of the intraocular implant, the IOLs must have strict quality and performance features. IOL designs must fulfil the strict requirements in terms of the optical performance (resolution efficiency or modulation transfer function) following the requirements set out by the International Standards ISO (11979-2:2014), and in terms of mechanical properties (compression force, dimension tolerance, and dynamic fatigue durability), following the guidelines specifies in the International Standards ISO (11979-3:2012). Several studies have experimentally and numerically evaluated the biomechanical properties

* Correspondence to: Calle María de Luna, 50018, Edificio Betancourt, University of Zaragoza, Spain.
E-mail address: iulen@unizar.es (I. Cabeza-Gil).

https://doi.org/10.1016/j.jmbbm.2020.104165
Received 31 December 2019; Received in revised form 11 August 2020; Accepted 23 October 2020
Available online 27 October 2020
1751-6161/

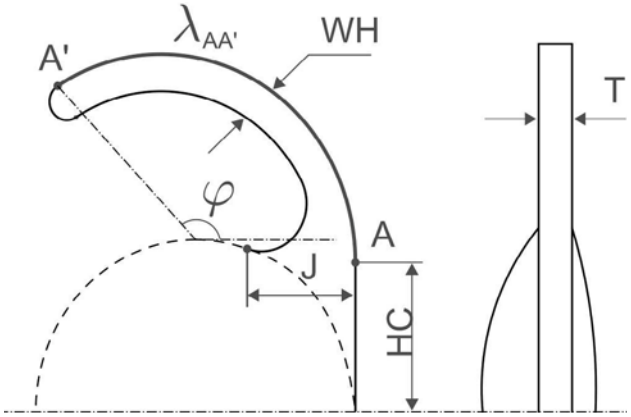

Fig. 1. Geometry of the IOLs under investigation.

of different IOLs (Lane et al., 2004; Bozukova et al., 2015; Remón et al., 2018; Lane et al., 2019).

In our previous study (Cabeza-Gil et al., 2019), we performed a numerical study through finite element method (FEM) to determine the effect on the biomechanical stability of haptic geometry in C-loop IOLs, based on the methodology of design of experiments (Montgomery, 2001). We suggested that stiffer designs provide a worse response within the capsular bag, according to the procedure described by ISO (11979-3:2012). Hence, we designed five IOLs with the same optic, classified in two patterns, stiff and flexible, which depend mainly on the haptic–optic junction, see Fig. 1. The aim of the present work was to confirm experimentally the same tendency of the numerical results. For that purpose, five IOLs were manufactured and tested on a commercial device MFC-1385-IOL (AMCC, France). The experimental and numerical results were correlated, analysing the following mechanical biomarkers: compression force, axial displacement, angle of contact, decentration and tilt. Moreover, from the *in vitro* results, the optical properties were evaluated using a PMTF (Lambda-X, Belgium) system according to the procedure described by ISO (11979-2:2014). The effect of IOL misalignment, tilt and axial displacement on the imaging quality was evaluated.

The results obtained in this study could be a milestone in the design of intraocular lenses. The numerical model could help manufacturers during the design phase and increase the predictability of cataract surgery. In this way, a major advance in time and cost savings could be added using the proposed methodology.

2. Materials and methods

2.1. Intraocular lenses

Five 1-piece C-loop IOLs with different haptic design were manufactured according to the results obtained in our previous work (Cabeza-Gil et al., 2019). The geometry of the haptics was parametrised by six factors: the length ($\lambda_{AA'}$), the width (WH), the thickness (T) and the opening angle (φ) of the haptic, the start of the curvature haptic (HC), and the haptic–optic junction (J), see Fig. 1 and Table 1. Based on the haptic–optic junction (J), the models *A*, *C*, and *E* were classified as flexible models while the models *B* and *D* as stiff ones. All models presented an overall diameter of 13.00 mm, except for Model *E*, which had 11.50 mm. The optic body diameter was 6.00 mm.

All the IOLs were designed with an aberration-free aspheric optic design at the anterior lens surface. IOLs were manufactured in hydrophobic acrylic material Benz HF-1.2 Universal Blank (Benz Research and Development, USA), with a dioptric power of 20.00 dioptres (D). The refractive index is n = 1.485 at the design wavelength λ_0 = 546 nm. The radii of curvature for the front and back surfaces were 11.49 mm and −21.00 mm, respectively. To design the aspheric IOL, a numerical model of a pseudophakic eye was implemented in an optical analysis software OSLO EDU (Lambda Research Corporation, USA). The model eye was based on the Navarro et al. (1985) schematic eye where the crystalline lens was replaced by the IOL. The aberration free design was intended to avoid adding fourth-order Zernike spherical aberration (Z04).

Table 1
Values of the geometrical parameters of the IOLs under investigation.

IOLs	Geometrical parameters					
	$\lambda_{AA'}$ [mm]	WH [mm]	φ [°]	J [mm]	HC [mm]	T [mm]
#A	8.80	0.40	115	0.60	2.30	0.40
#B	8.80	0.40	115	1.80	2.30	0.40
#C	8.80	0.65	115	0.60	2.30	0.40
#D	8.80	0.65	115	1.80	2.30	0.40
#E	8.80	0.40	135	0.60	2.50	0.40

The IOLs were manufactured by a lathe-milling process without polishing step, see Fig. 2. Differences between the theoretical design and the manufactured IOL geometrical parameters were lower than 0.3 mm as measured with a Leica S6D LED microscope (Leica Camera AG, Germany). The haptic design is the differentiating factor between these five models.

2.2. Material characterisation

In order to evaluate the mechanical response of the hydrophobic acrylate material of the IOLs, uniaxial tensile and compression tests were conducted under displacement control on an INSTRON 5548 Electroplus microtester with a 150.00 N full scale load cell. Three dogbone flat samples with a gauge length of 7.50 mm, a width of 1.00 mm and an overall length of 15.00 mm were used for the tensile test. Whereas three disks of 3.00 mm thickness and 15.00 mm of diameter were used for the compression test. Before the experiments, all samples were submerged for 72 h in a saline bath at 35 °C.

Samples were subjected to four loading/unloading cycles up to 20% deformation in compression and to 10% in tensile stress, since its breaking point was close to this value. The velocity rate of the clamps for all samples was v = 1 mm/min, assuming a quasi-static situation. Samples were kept submerged during the entire experiment. With the data recorded during the test, the stretch was calculated as $\lambda = \frac{L_0+\triangle L}{L_0}$, where L_0 is the initial length between clamps and $\triangle$ L is the clamp displacement. Finally, the nominal stress or first Piola–Kirchhoff stress was obtained as $P = \frac{N}{CSA}$, where N is the applied load and CSA is the cross-section of the sample.

2.3. In silico compression test

Numerical simulations of the mechanical stability of the IOL during a compression test were performed using Abaqus 6.14 (Dassault Systèmes, France) according to ISO 11979-3. The biomechanical stability was evaluated through five main responses: *compression force* –mN–, *axial displacement* –mm–, *tilt* –degrees, °– , *contact angle* –degrees, °– and *decentration* –mm–. Moreover, thanks to the finite element (FE) model, the actual *contact area* –mm^2–, a more accurate measurement than the contact angle, and the *strain energy*, –μJ–, could be measured.

In this compression test, the IOL is placed between two clamps (with a curvature radius of 5.00 mm) and compressed to measure its mechanical stability. The FE model is shown in Fig. 3a. A 'hard' contact relationship was used to minimise penetration between the contact surfaces and a friction coefficient of μ = 0.2 was considered due to the high cohesiveness of the material seen in the experimental tests. A node-to-surface contact was used to ease convergence. The material considered for the lens was assumed to be hyperelastic and isotropic while the clamps were considered as rigid solids. The clamps

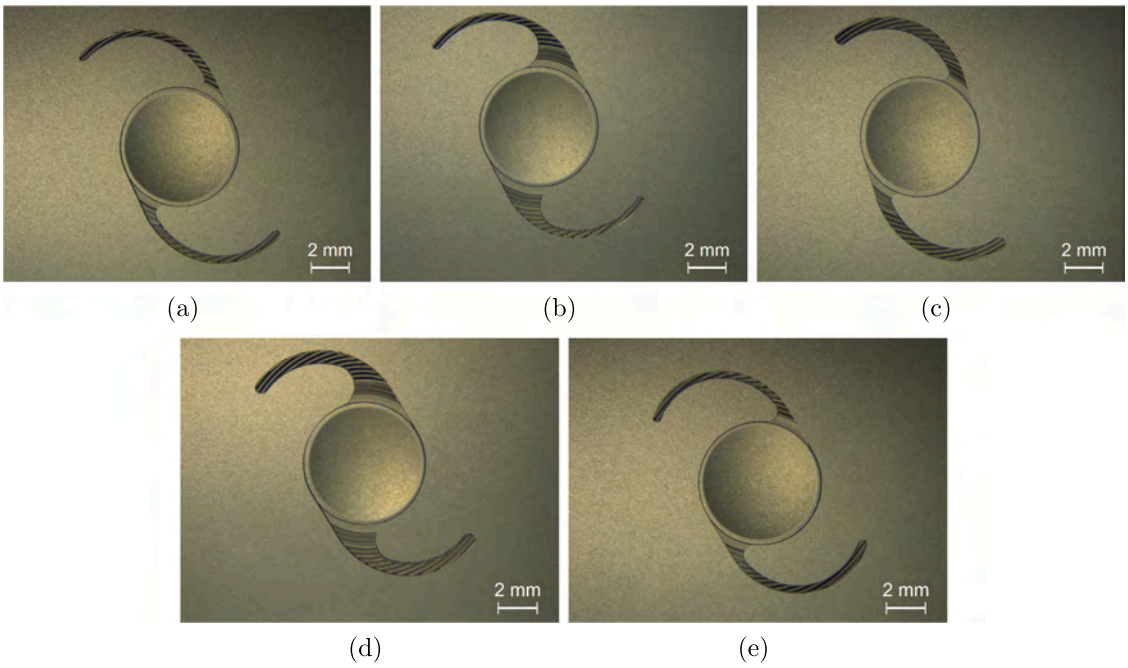

Fig. 2. Images of the manufactured lenses taken with Leica S6D LED. (a) Model *A*. (b) Model *B*. (c) Model *C*. (d) Model *D*. (e) Model *E*. An anti-stick profile was included in the haptic design to provide better unfolding when inserting the lenses.

are initially separated a distance greater to the overall dimension of the IOL to allow its gentle positioning without introducing pretension (see Fig. 3(a)). Then, the right clamp is displaced until a compression diameter of 9.00 mm while the left clamp remains fixed (see Fig. 3b–c). The biomechanical response was evaluated over its entire range. The standard ISO 11979-3 establishes that five key points must be recorded in order to determine the stability of the IOL (see Fig. 3b–c).

2.4. *In vitro* compression test

In vitro tests were performed using the MFC-1385-IOL device (AMCC, France), see Fig. 4. The IOLs under investigation were compressed at a diameter of 10.00 mm following the standard ISO 11979-3 specifications for the intended use in the capsular bag. The clamps of the device are made of High-Density Polyethylene (HDPE) and the IOLs compressed in clamps were submerged in a saline solution at 35 ± 2 °C, simulating in vivo conditions. The device provides directly the compression force at a 10.00 ± 0.10 mm haptic compression. A USB camera was used to capture the images before and after the compression test. From these images the axial displacement, tilt and contact angle were measured with AutoCAD software (Autodesk, USA). All measurements were performed under identical conditions. Five IOLs of each group were tested sequentially.

2.5. *In vitro optical performance*

To study the effect of misalignment (decentration), tilt and axial displacement on the imaging quality, the optical properties were evaluated experimentally using the optical bench PMTF (Lambda-X S.A., Belgium). This device follows the requirements of ISO standard 11979-2. The equipment disposes of two model corneas with different values of spherical aberrations (SA): The ISO1 model cornea with zero spherical aberration and the ISO2 model cornea with +0.280 μm SA for 5.00 mm pupil aperture. In this study, ISO2 was used as a cornea. The *in vitro* results of the mechanical biomarkers at 10.00 mm were introduced as input parameters to evaluate the optical performance. To do this, IOLs were first tilted, then decentered and finally, the CCD camera was moved axially to simulate the axial displacement of the IOL. In this situation, the Modulation Transfer Function (MTF) at 100 cycles per degree with a 3.00 mm aperture pupil was measured, and images of the 1951 USAF target through the artificial eye were taken.

2.6. *Statistical analysis*

Descriptive statistics were used for all objective measurements with the mean and standard deviation (SD) for the *in vitro* and *in silico* results. An ANOVA analysis for all groups was performed. All *in vitro* and *in silico* pairs were also analysed. All the analysis was performed using Matlab v2020a (MathWorks, USA). A $p_{value} \leq 0.05$ was considered as statistically significant.

3. Results

3.1. *Material characterisation*

After analysing the nominal stress–strain curves obtained in the uniaxial tests, a phenomenological behaviour which describes the experimental response at a macroscopic level was necessary to define. A hyperelastic model was used to reproduce the large deformations. A study was carried out to select the hyperelastic model that best fitted to the experimental data. From this study, the hydrophobic acrylate IOLs material was adjusted by the Ogden strain energy function with N=4:

$$\Psi = \sum_{i=1}^{N} \frac{2\mu_i}{\alpha_i}(\lambda_1^{-\alpha_i} + \lambda_2^{-\alpha_i} + \lambda_3^{-\alpha_i} - 3) + \frac{1}{D_1}(J^{el} - 1)^2 \quad (1)$$

with $\lambda_{1,3}$, being the deviatoric principal stretches. μ, α, and D_1 are the material constants and their corresponding values are: $\mu_1 = -61.87$ MPa, $\mu_2 = 30.25$ MPa, $\mu_3 = 61.67$ MPa, $\mu_4 = -29.42$ MPa, $\alpha_1 = 10.72$, $\alpha_2 = 13.43$, $\alpha_3 = 5.54$, $\alpha_4 = 4.24$, $D_1 = 0.19$ MPa^{-1}. The experimental and numerical nominal stress–strain curves were represented in Fig. 5. As can be seen, the material exhibits different tensile and compression behaviour.

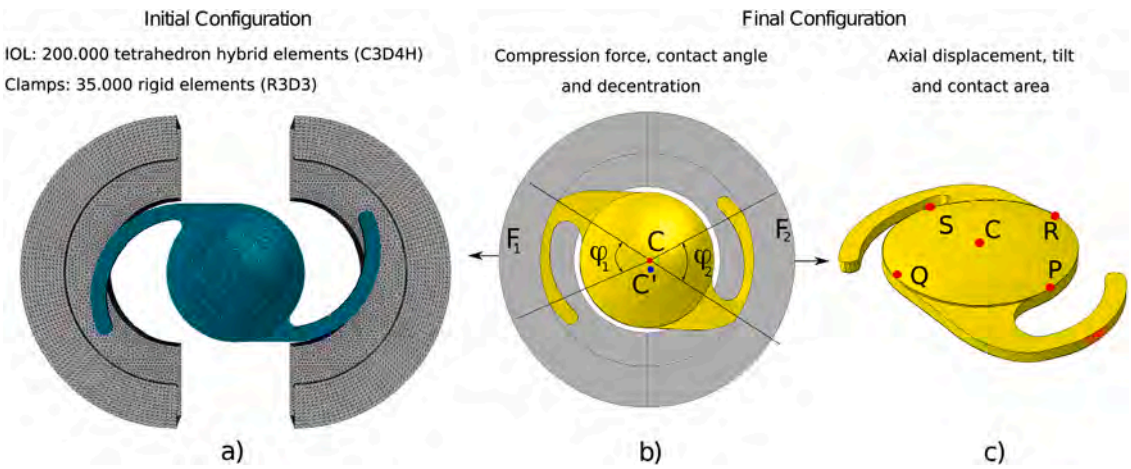

Fig. 3. *In silico* model of the compression test. (a) Mesh of the FE model; b) Measurement of the IOL's compression (or reaction) force, angle of contact, and decentration. Force is given by the mean force in the haptics ($F = \frac{F_1+F_2}{2}$). Angle of contact is given by the sum between (γ_1) and (γ_2). Decentration is the absolute distance between C and C′ (red and blue point, respectively). (c) Representation of the key points (in red) used for the evaluation of the tilt (S, R, Q, P) and the axial displacement (C). The contact area is depicted in red in the front part of the haptic and is calculated internally by Abaqus v6.14.

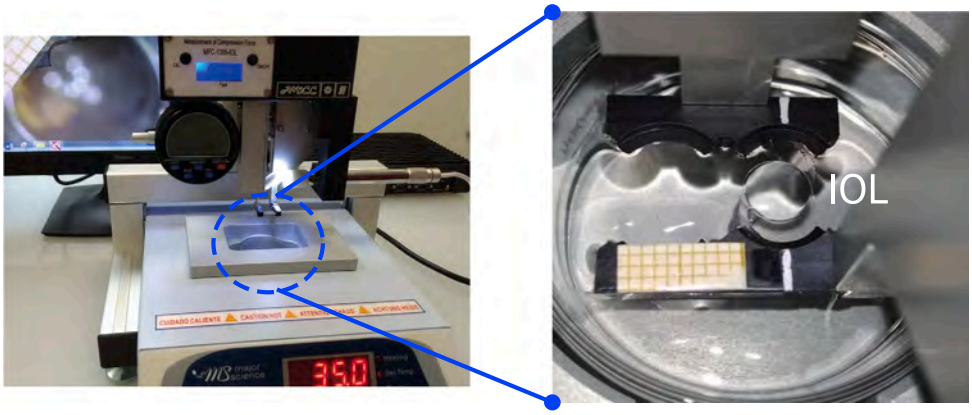

Fig. 4. MFC-1385-IOL device used for *in vitro* compression test.

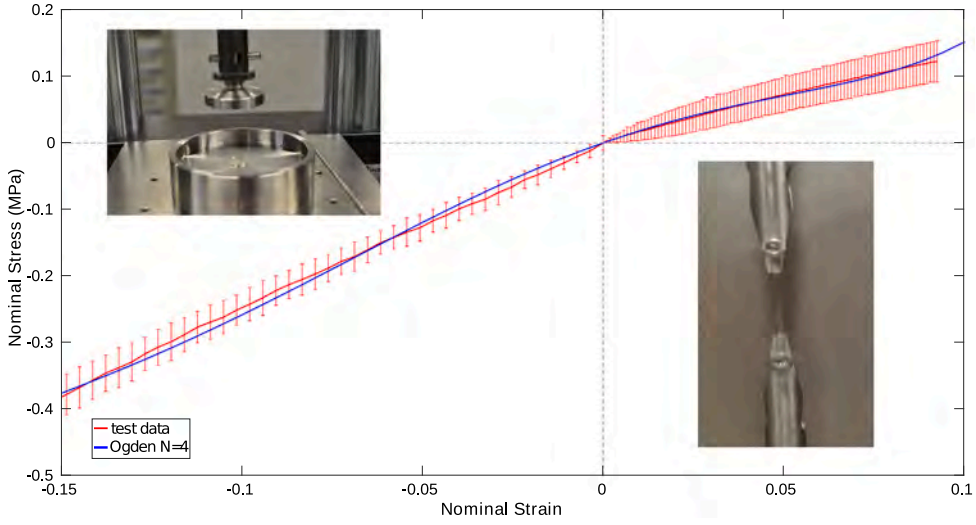

Fig. 5. Experimental and numerical hydrophobic acrylate material behaviour.

3.2. Biomechanical stability

In order to evaluate the biomechanical stability of the five C-Loop IOLs under investigation, the compression force, the axial displacement, the tilt, the contact angle and the decentration were analysed *in vitro* and *in silico*. Fig. 6 shows the corresponding results for an IOL compression diameter of 10.00 mm. As the MFC-1385-IOL device measures the IOL response at a compression diameter of 10.00 ± 0.10 mm, the mean

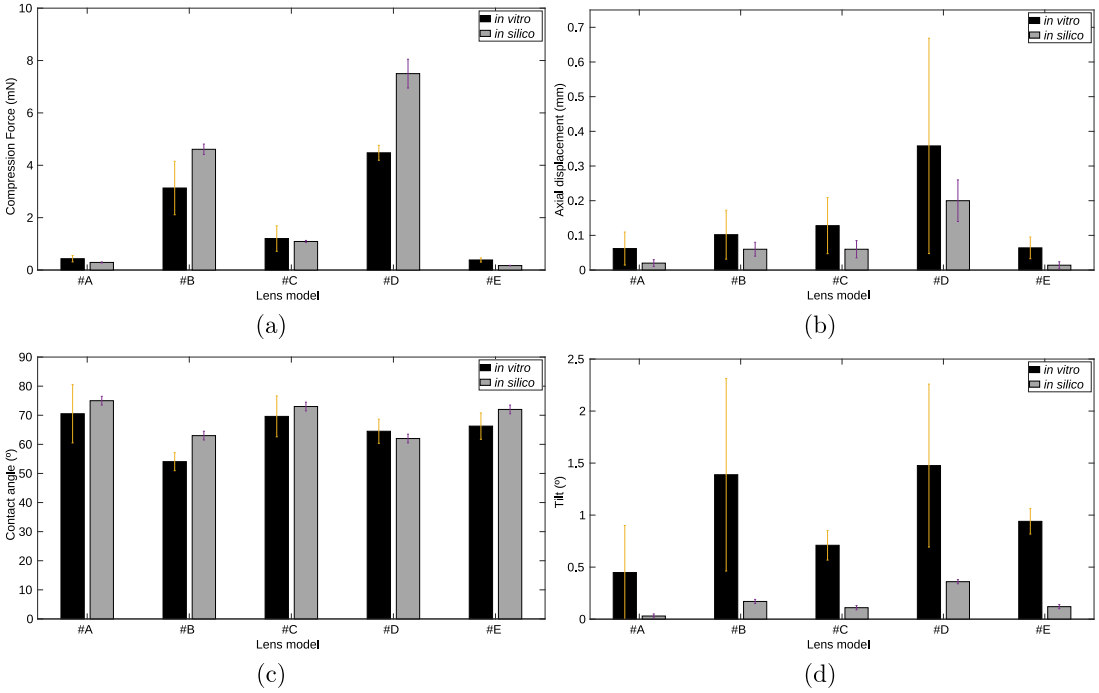

Fig. 6. Comparative values of the biomechanical stability between *in vitro* (black) and *in silico* (grey) when the clamps are closed at 10 mm: (a) Compression force; (b) Axial displacement; (c) Haptic-clamp angle of contact; (d) Tilt.

and SD *in silico* results were calculated averaging the response within the device tolerance.

Regarding the compression force, see Fig. 6a, there is a statistically significant difference ($p_{value} < 0.05$) between the stiff and flexible models. Models *B* and *D*, classified as the stiff ones, present a greater *in vitro* response, 3.13 ± 1.02 and 4.47 ± 0.28 mN, respectively, whereas the mean compression force for the flexible models *A* and *E* was 0.41 ± 0.09 mN. Model *C*, which has a higher width of the haptic than the other flexible models, presents a compression force of 1.20 ± 0.48 mN. The *in silico* response is comparable to *in vitro* results, but providing a greater compression force of 4.62 ± 0.21 and 7.52 ± 0.55 mN for models *B* and *D*, respectively. Nevertheless, there is not a statistically significant difference between *in vitro* and *in silico* results ($p_{value} > 0.05$), except for model *D* ($p_{value} < 0.05$).

In terms of the axial displacement, see Fig. 6b, model *D* presents the highest *in vitro* value and deviation, resulting in 0.35 ± 0.31 mm, opposed to 0.19 ± 0.05 mm provided *in silico*. The other models (*A*, *B*, *C*, and *E*) barely presented axial displacement, neither *in vitro* nor *in silico*.

Concerning the angle of contact, see Fig. 6c, there is not statistically significant difference between *in vitro* and *in silico* results ($p_{value} > 0.05$). However, there was a statistically significant difference ($p_{value} < 0.05$) between the stiff models *B* and *D*, with a mean value of 56.25 ±3.61° and the flexible IOL designs (*A*, *C*, and *E*), 68.45 ±7.86°.

Finally, in the tilt response, see Fig. 6d, there is a statistically significant difference between *in vitro* and *in silico* results ($p_{value} < 0.05$). The numerical results of the tilt are approximately zero. Moreover, for the *in vitro* results there is a statistically significant difference between the stiffest models (*B* and *D*) and the flexible ones (*A*, *C*, and *E*). The mean *in vitro* value of the IOL designs (*B* and *D*) is 1.43 ±0.85° whereas for the flexible IOL designs is 0.73 ±0.27°. The mean decentration is 0.23 ± 0.04 mm and 0.08 mm for *in vitro* and *in silico*, respectively.

Fig. 7 shows the evolution of compression force, axial displacement contact area and strain energy as a function of the IOL diameter compression. Models *B* and *D* were only stable up to a compression diameter of 9.35 mm. The compression force variation, see Fig. 7a, when the haptic was compressed to 10.00 mm, ranged from 7.52 mN for the model *D* to 0.30 mN for the model *A*. The axial displacement variation, see Fig. 7b, when the haptic was compressed to 10.00 mm, ranged from 0.19 mm for the model *D* to 0.01 mm for the models *A*, *B* and *E*. For model *D*, the axial displacement increases exponentially from 10.40 up to 9.85 mm and is correlated with the other responses, while model *B* starts to present an exponential behaviour from an IOL diameter compression of 10.00 mm. The stiff models (*B* and *D*) present a higher contact area, around 0.55 mm^2 along the entire response, see Fig. 7c, whereas the flexible models present a contact area of 0.15 mm^2. Lastly, the strain energy follows the same pattern as the compression force, reaching a strain energy of 5.27 μJ for model *D* at 9.85 mm.

3.3. In vitro optical performance

Fig. 8 shows the images of the USAF with a 3.00 mm diameter pupil for all IOLs under investigation. The images were taken on-axis and off-axis with a combination of misalignment and tilt (top row) and combination of misalignment, tilt and axial displacement (bottom row). As can be seen, model *B* presents the worst image quality when the axial displacement was set to 0. However, when the axial displacement was considered, model *D* had the worst image quality. Fig. 9 shows the experimental on axis and off axis MTF results. On-axis MTFs was above to 0.43 for all models (value specified at the ISO 11979-2). When the displacement parameters were considered, MTF value falls below 0.43 for all models of IOL; when the axial displacement was set to 0, MTF value falls below 0.43 for models *B*, *C* and *D*. The results were consistent with the USAF images.

4. Discussion

The ISO (11979-3:2012) specifies requirements and test methods for certain mechanical properties of IOLs intended for capsular bag placement. The mechanical properties are essential to guarantee a good stability inside the capsular bag avoiding decentration, axial displacement, tilt or rotation that affect the visual performances after cataract surgery (Garzón et al., 2015; Mihálta et al., 2018). The main goal of this study was to design an aberration-free spherical IOL and to study

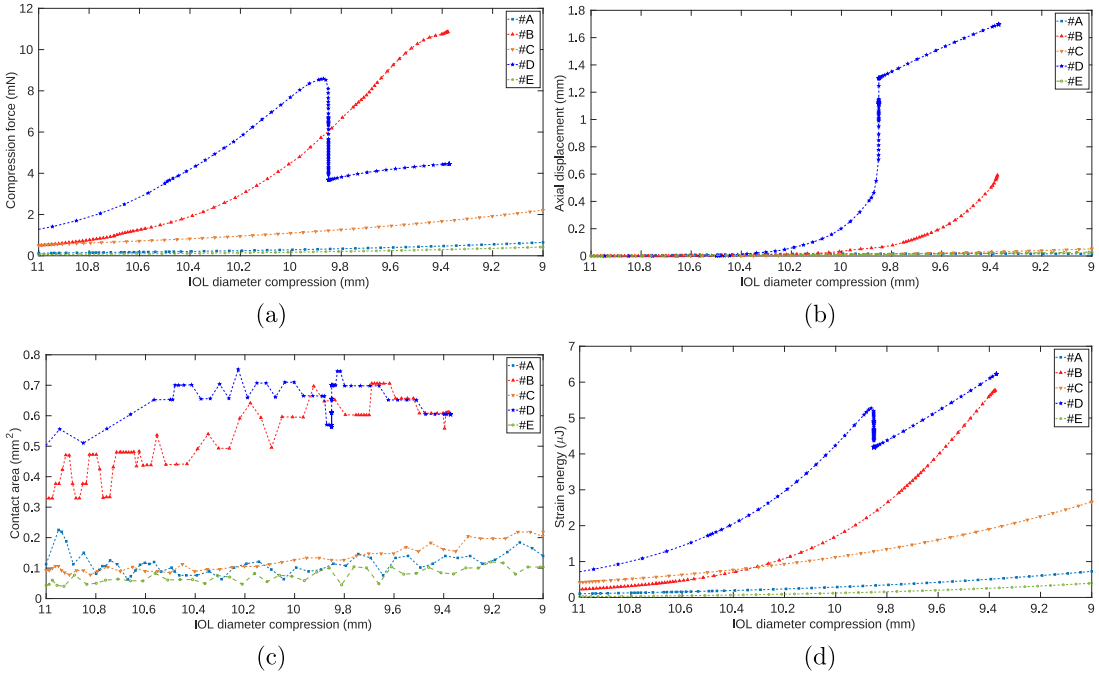

Fig. 7. *In silico* results of the compression force (a), axial displacement (b), contact area (c) and the strain energy (d) vs the IOL diameter compression (mm) for all IOLs analysed.

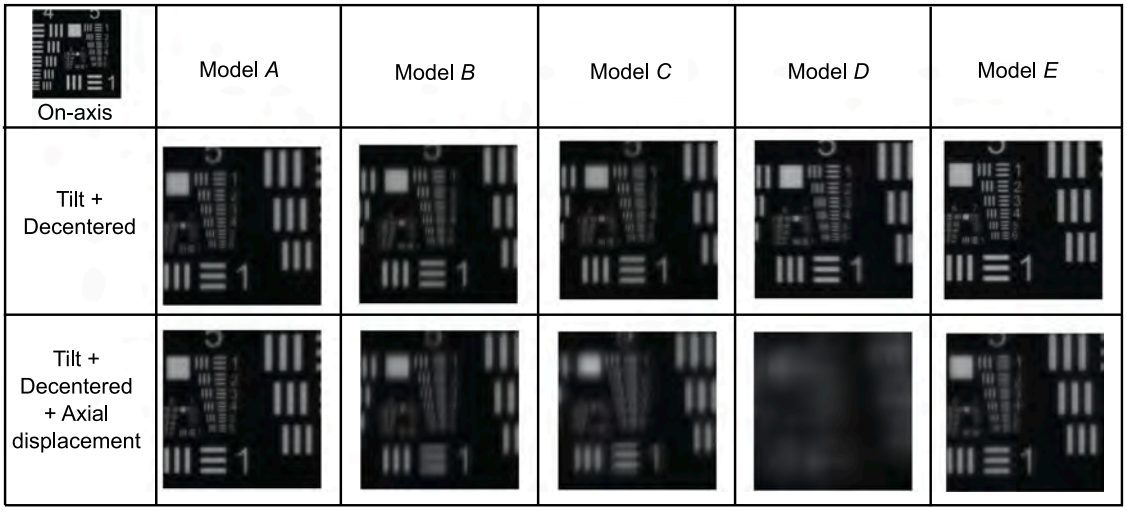

Fig. 8. The 1951 USAF test images of the different IOLs models for on-axis, tilt and decentered, and the worst-case scenario position for all the IOLs under investigation.

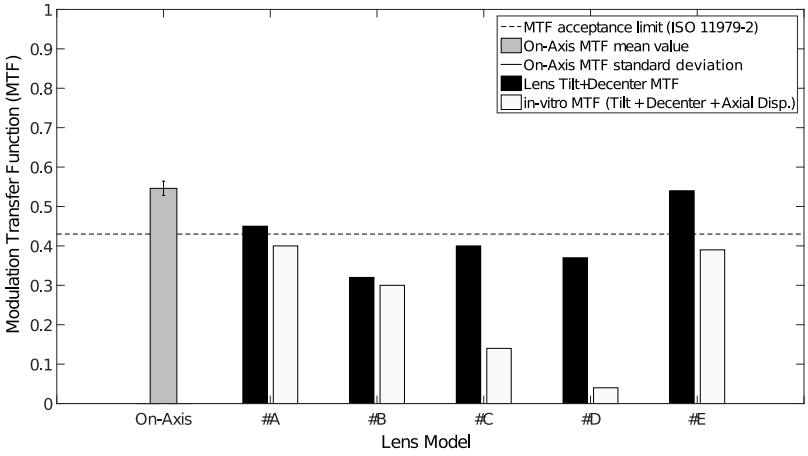

Fig. 9. MTF deviation compared to the On-axis MTF value and the MTF obtained from the results *in vitro*, measured in the PMTF instrument.

the influence of haptic geometry on the optical quality. To do this, 5 hydrophobic IOLs with different haptic design were manufactured (see Fig. 2) and the biomechanical stability was compared numerically and experimentally. The IOLs were classified as stiff (models *B* and *D*) and flexible designs (models *A*, *C*, and *E*) depending on their haptic geometry. Previously, we evaluated the biomechanical properties (Cabeza-Gil et al., 2019) *in silico* of these models of IOLs and we found that the stiffer IOLs designs tend to offer a worse stability than flexible ones. A comparison between *in vitro* and *in silico* results was performed.

It can be stated that these results have provided undeniable evidence of a correlation between the *in vitro* and *in silico* results, see Fig. 6. Based on the high deviation in compression force and axial displacement presented in the *in vitro* tests, to make a more accurate comparison, they were compared with the numerical results within the MFC-1385-IOL device tolerance. The deviation in the *in vitro* results can be explained by the numerical response, see Fig. 7a and Fig. 7b, which shows a high sensitivity of the responses as function of the IOL diameter compression.

The compression force showed the same trend *in vitro* and *in silico*. However the *in silico* compression force for the models *B* and *D* were slightly higher than those measured *in vitro*. Models *B* and *D* were stable up to 9.35 mm, what suggests that a lower IOL diameter compression could compromise the stability of these IOLs. Moreover, the strain energy was directly correlated with the compression force, see Fig. 7a and Fig. 7d. Bozukova et al. (2015) also found that the *in silico* radial compression forces were generally higher than those measured *in vitro*.

Experimentally, the *in vitro* axial displacement showed higher values than *in silico* results. Model *D* presents the greatest axial displacement, resulting in 0.35 ± 0.31 mm *in vitro* conditions. Their high deviation can be explained observing Fig. 7a and Fig. 7b, which shows that the critical compression diameter of this IOL is close to 10.00 mm, where the *in vitro* and *in silico* results were compared. Recently, Lane et al. (2019) found an axial displacement at 10.00 mm ranging from −0.01 mm for the Acrysof SN60WF to 0.68 mm for the enVista MX60.

Concerning the haptic-clamp angle of contact, the *in vitro* results were quite similar to the *in silico* results. The stiffest models seem to have a lower angle of contact. The actual contact area was measured numerically, which cannot be measured experimentally, and the results showed that the stiffest models presented a higher contact area, which seems to be correlated with the compression force. This inconsistency shows that the angle of contact may not be the right measurement since it is a subjective measurement and provides not so accurate results.

In silico optic tilt was generally lower than those measured *in vitro*. Models *B* and *D* present a mean optic tilt of 1.43 ±0.85° *in vitro* conditions and in the other models the mean optic tilt was 0.73 ±0.27° in the same conditions. Lane et al. (2019) found experimentally an optic tilt between 0.5° to 1.2° for all evaluated IOLs. From an operator's perspective, those experimental values are practically 0°, so it could be said that also the *in vitro* and *in silico* tilt is correlated. These results suggests that flexible IOL designs offer a better biomechanical stability than stiffer models, which is consistent with the findings in previous studies (Bozukova et al., 2013; Lane et al., 2019). Last but not least, the optical performance, evaluated experimentally, showed small changes in the MTF and image quality (USAF) when the magnitudes of displacement parameters (only tilt and decentered) are considered. However, with axial displacement, there is a considerable loss of optical quality. It allowed us to verify that the mechanical biomarkers can predict the optical performance.

The large deviation measured *in vitro* for the different main responses, particularly, for the axial displacement and optic tilt, can be also explained by some noisy factors such as temperature; IOL placement, which could affect the contact areas; or even the subjective measures taken by the operator. Previously, Lane et al. (2004, 2019), found also a great variability in their experimental work, which suggests the need of a standardised biomechanical testing procedure to compare different IOL designs.

One of the limitations of the *in vitro* measurements is that only one IOL diameter compression (10.00 mm) can be tested while the clinical outcomes might depend on the capsular bag size (Garzón et al., 2015). In this study, the biomechanical responses were evaluated numerically for different IOL diameters compression simulating different capsular bag sizes, see Fig. 7. As can be seen, a lower simulated capsular bag size induced higher compression force and axial displacement, being the highest value for the models *B* and *D*. In conclusion, the FE model proposed can reproduce faithfully the compression test, ISO (11979-3:2012). Moreover, it can be useful in the design phase to the manufacturers, reducing costs and time by exploring a feasible space of solutions during the product design process and before manufacturing. Further studies should be carried out to analyse how the compression test can predict the behaviour of the lens in the capsule.

CRediT authorship contribution statement

I. Cabeza-Gil: Methodology, Software, Formal analysis, Writing - original draft. **J. Pérez-Gracia:** Investigation, Resources, Writing - original draft. **L. Remón:** Conceptualization, Supervision, Writing - reviewing & editing. **B. Calvo:** Conceptualization, Supervision, Writing - reviewing & editing.

Declaration of competing interest

The authors declare that they have no known competing financial interests or personal relationships that could have appeared to influence the work reported in this paper.

Acknowledgements

The authors gratefully acknowledge research support from the Spanish Ministerio de ciencia, innovacion y universidades (Grant DPI2017-84047-R) and the Department of Industry and Innovation (Government of Aragon), Spain through the research group Grant T24-20R (cofinanciado con Feder 2014–2020: Construyendo Europa desde Aragon). Part of the work was performed by the ICTS 'NANBIOSIS' specifically by the High-Performance Computing Unit (U27) of the CIBER in Bioengineering, Biomaterials & Nanomedicne (CIBER-BBN at the University of Zaragoza). Moreover, authors acknowledge AJL Ophthalmic S.A. for manufacturing the proofs of concept of IOLs in this study. I. Cabeza-Gil and J.Perez-Gracia were supported by the Spanish Ministry of Economy and Competitiveness, PRE2018-084021 and DI-16-08888, respectively.

References

Alió, J., Plaza-Puche, A., Javaloy, J., Ayala, M., Vega-Estrada, A., 2013. Clinical and optical intraocular performance of rotationally asymmetric multifocal IOL plate-haptic design versus c-loop haptic design. J. Refract. Surg. 29 (4), 252–259.

Bozukova, D., Pagnoulle, C., Jérôme, C., 2013. Biomechanical and optical properties of 2 new hydrophobic platforms for intraocular lenses. J. Cataract. Refract. Surg. 39 (9), 1404–1414.

Bozukova, D., Werner, L., Mamalis, N., Gobin, L., Pagnoulle, C., Floyd, A., Liu, E., Stallings, S., Morris, C., 2015. Double-c loop platform in combination with hydrophobic and hydrophilic acrylic intraocular lens materials. J. Cataract. Refract. Surg. 41 (7), 1490–1502.

Cabeza-Gil, I., Ariza-Gracia, M.Á., Remón, L., Calvo, B., 2019. Systematic study on the biomechanical stability of c-loop intraocular lenses: Approach to an optimal design of the haptics. Ann. Biomed. Eng..

Chan, E., Mahroo, O.A.R., Spalton, D.J., 2010. Complications of cataract surgery. Clin. Exp. Opt. 93 (6), 379–389.

Chang, D., 2008. Comparative rotational stability of single-piece open-loop acrylic and plate-haptic silicone toric intraocular lenses. J. Cataract. Refract. Surg. 34 (11), 1842–1847.

Choi, M., Lazo, M., Kang, M., Lee, J., Joo, C., 2018. Effect of number and position of intraocular lens haptics on anterior capsule contraction: a randomized, prospective trial. BMC Ophthalmol. 18 (1).

Chua, W., Yuen, L., Chua, J., Teh, G., Hill, W., 2012. Matched comparison of rotational stability of 1-piece acrylic and plate-haptic silicone toric intraocular lenses in asian eyes. J. Cataract. Refract. Surg. 38 (4), 620–624.

Crnej, A., Hirnschall, N., Nishi, Y., Gangwani, V., Tabernero, J., Artal, P., Findl, O., 2011. Impact of intraocular lens haptic design and orientation on decentration and tilt. J. Cataract. Refract. Surg. 37 (10), 1768–1774.

Garzón, N., Poyales, F., de Zárate, B.O., Ruiz-García, J., Quiroga, J., 2015. Evaluation of rotation and visual outcomes after implantation of monofocal and multifocal toric intraocular lenses. J. Refract. Surg. 31 (2), 90–97.

ISO, 11979-2:2014. Ophthalmic implants. Intraocular lenses. Part 2: Optical properties and test methods. BSI Standards Limited.

ISO, 11979-3:2012. Ophthalmic implants. Intraocular lenses. Part 3. Mechanical properties and test methods. BSI Standards Limited.

Lane, S., Burgi, P., Milios, G., Orchowski, M., Vaughan, M., Schwarte, E., 2004. Comparison of the biomechanical behavior of foldable intraocular lenses. J. Cataract. Refract. Surg. 30 (11), 2397–2402.

Lane, S., Collins, S., Das, K.K., Maass, S., Thatthamla, I., Schatz, H., Noy, S.V., Jain, R., 2019. Evaluation of intraocular lens mechanical stability. J. Cataract. Refract. Surg. 45 (4), 501–506.

Miháltz, K., Lasta, M., Burgmüller, M., Vécsei-Marlovits, P., Weingessel, B., 2018. Comparison of two toric IOLs with different haptic design: Optical quality after 1 year. J. Ophthalmol. 2018, 1–7.

Montgomery, D., 2001. Design & Analysis of Experiments, fifth ed. John Wiley, New York.

Nagy, Z., Kránitz, K., Takacs, A., Miháltz, K., Kovács, I., Knorz, M., 2011. Comparison of intraocular lens decentration parameters after femtosecond and manual capsulotomies. J. Refract. Surg. 27 (8), 564–569.

Navarro, R., Santamaria, J., Bescos, J., 1985. Accommodation-dependent model of the human eye with aspherics. J. Opt. Soc. Amer. A 2 (8), 1273–1281.

Pérez-Merino, P., Marcos, S., 2018. Effect of intraocular lens decentration on image quality tested in a custom model eye. J. Cataract. Refract. Surg. 44 (7), 889–896.

Prinz, A., Neumayer, T., Buehl, W., Vock, L., Menapace, R., Findl, O., Georgopoulos, M., 2011. Rotational stability and posterior capsule opacification of a plate-haptic and an open-loop-haptic intraocular lens. J. Cataract. Refract. Surg. 37 (2), 251–257.

Remón, L., Siedlecki, D., Cabeza-Gil, I., Calvo, B., 2018. Influence of material and haptic design on the mechanical stability of intraocular lenses by means of finite-element modeling. J. Biomed. Opt. 23 (03), 1.

Schmidbauer, J.M., Escobar-Gomez, M., Apple, D.J., Peng, Q., Arthur, S.N., Vargas, L.G., 2002. Effect of haptic angulation on posterior capsule opacification in modern foldable lenses with a square, truncated optic edge. J. Cataract. Refract. Surg. 28 (7), 1251–1255.

Vock, L., Georgopoulos, M., Neumayer, T., Buehl, W., Findl, O., 2007. Effect of the hydrophilicity of acrylic intraocular lens material and haptic angulation on anterior capsule opacification. Br. J. Ophthalmol. 91 (4), 476–480.

Vounotrypidis, E., Lackerbauer, C., Kook, D., Dirisamer, M., Priglinger, S., Mayer, W., 2018. Influence of total intraocular lens diameter on efficacy and safety for in the bag cataract surgery. Oman. J. Ophthalmol. 11 (2), 144–149.

Wirtitsch, M., Findl, O., Menapace, R., Kriechbaum, K., Koeppl, C., Buehl, W., Drexler, W., 2004. Effect of haptic design on change in axial lens position after cataract surgery. J. Cataract. Refract. Surg. 30 (1), 45–51.

Zvorničanin, J., Zvorničanin, E., 2018. Premium intraocular lenses: The past, present and future. J. Curr. Ophthalmol. 30 (4), 287–296.